A New Framework to Extract Heart Rate Information from Photoplethysmographic (PPG) Signals with Strong Motion Artifacts

Zi-Hao Zhang, Jian Liu, Xiao-Yue Wu, Chao-Ying Wang and Ran Yang
School of Mobile Information Engineering
Sun Yat-sen University, Zhuhai, P. R. China, 519082
Email: zhzihao2@mail2.sysu.edu.com

***Abstract*—Photoplethysmography (PPG) as a non-invasive measurement of physiological information, has broad application prospects. However, PPG signals can be interfered by movement seriously. Therefore, how to extract information from PPG with strong motion artifacts is a severe problem to be solved. In this paper, we proposed a new framework to extract heart rate (HR) information from PPG signals with strong motion artifacts. In this framework, Singular Spectrum Analysis, Real-time Clustering, Frequency Points Selection and Prediction, Multiple-way Selection are the key procedures. The experiment shows that the proposed framework can achieve good performance in terms of both robustness and high precision.**

***Index Terms*—Photoplethysmograph (PPG); Heart Rate Extraction; Motion Artifacts; Singular Spectrum Analysis (SSA); Real-time Clustering; Error Recovery; Wearable Computing**

I. Introduction

Physiological data plays an irreplaceable role in clinical treatment, among which, Heart rate (HR) can be used to monitor cardiovascular and respiratory disease, and HR monitoring for fitness is important for exercisers to control their training load. Thus, it will be of great help if the health information of patients can be assessed in real time and monitored continuously through wearable medical devices.

Photoplethysmography (PPG) is such a technique that is extremely suitable for wearable sensing, since it provides useful cardiovascular and respiratory information, such as oxygen saturation, blood pressure and cardiac output, without puncturing the skin.

However, the current technique can not meet the practical requirements, especially in the case of intensive exercises. The PPG signal can be easily corrupted by motion artifacts, and the information contained in the PPG signals will be distorted. Since clinical applications require a clean and enhanced signal for feature extraction, analysis, and monitoring, the motion artifacts must be removed.

A. Related Work

Heart rate (HR) monitoring is important in many aspects, including clinical applications and exercise. Photoplethysmography(PPG) is often used non-invasively to make measurements at the skin surface due to its simplicity and low-cost [1]. However, PPG signal is sensitive to motion artifacts, thus, there are many signal processing techniques proposed to deal with motion artifacts.

During the last decades, several methods have been attempted to deal with motion artifacts, and they can be roughly classified into three ways: to construct a model for the ideal PPG signal or the noise; to recognize the feature of motion artifacts from the corrupted signal directly [2] [3]; to get the measurement of motion artifacts independently. We could get the context information by using additional on-body sensors or light resources, or by using accelerometers as a noise reference.

For methods that construct a model for the ideal PPG signal or the noise, it is first assumed that the motion artifacts are the linear addition to the PPG signal, and the raw signal can be reconstructed from the corrupted one [4] [5] [6]. However, the hypothesis was doubted [7], since it didn't match with experiment results. Then a methodology which purposed to reduce the motion artifacts, proposed a new model based on the inversion of a nonlinear physical artifacts [7] [8], which is more realistic. Although the methods could reduce the motion artifacts at a large extent, its limitation is also obvious. Since the model-based method has close connection with the design of the model, it cannot cope with all aspects in daily life [3]. Because of this limitation, we don't adopt it in our framework.

For methods that recognize the feature of motion artifacts from the corrupted signal directly, limitation is much smaller. In this kind of methods, the noise and the uncorrupted PPG signals will be separated using specific condition. For instance, Swedlow et al. identified a component of the signal as motion artifacts when the ratio of adjacent positive and negative peaks of the components is below a threshold [9]. However, it may lost a large amount of available information if the noises are moved directly, especially when the frequency of the corrupted part is similar to the uncorrupted one. To avoid this rick, we don't adopt it in our framework.

For methods that get the measurement of motion artifacts independently, many sensors are used to record motion artifacts. Among which, adaptive noise cancellation using accelerometers as a noise reference is popular [10].For example, a 2-D active noise cancellation has been tried using the directional accelerometer data for finger PPG sensor [11]. However, there are two main drawbacks of these methods. The one is that extra

hardware is asked for the noise reference. Fortunately, there are lots of smart-watch type devices today, which can carry the extra hardware without burden. The other is that, although three-axis accelerometer data truly reflect motion, researchers found no direct or high correlation between the acceleration data and the motion artifacts [12]. To solve this problem, more synthetic noise generation method is proposed, such as fast Fourier transform (FFT), singular value decomposition (SVD) and independent component analysis (ICA [13]]. In our framework, we only use three-axis accelerometer data as a supporting factor instead of a conclusive factor.

Moreover, most of the upper techniques were proposed for clinical scenarios, when small motions are performed and motion artifacts are not strong. Thus, this techniques may not suitable for intensive physical exercises. Moreover, most of the techniques record PPG data from fingertips or ears and few work records PPG signals from wrist. Although collecting PPG signals from wrist may get much more severe motion artifacts, it combines with wearable devices perfectly, which could promote user experience. Thus, it is efficient to propose a high-accuracy framework to extract HR from wrist-type PPG signals [14].

Recently, a novel framework termed TROIKA was proposed. TROIKA achieves HR extraction from the wrist-type PPG signals with strong motion artifacts in frequency domain. TROIKA introduces signal decomposition to remove the motion artifacts with the help of acceleration information. In TROIKA, singular spectrum analysis is applied. What's more, TROIKA introduces sparse signal reconstruction to get the high-resolution spectrum information, instead of Fast Fourier Transform (FFT), because of the serious leakage effect of FFT. TROIKA achieves good performance in the cases where PPG signals are seriously interfered by intensive physical exercise. However, we think there is still a need of a higher precision algorithm to HR extraction, which can get the physical information more exactly. In the meanwhile, sparse signal reconstruction requires large calculation amount relatively, which is a burden to mobile devices [14].

B. Our Work

This work focuses on the HR extraction from Wrist-Tpye Photoplethysmographic (PPG) Signals with strong motion artifacts. We deal with the PPG data fetched in the case where wearers perform intensive physical exercise, such as running, boxing, jumping and so on. In these cases, movements of wearer will interfere the PPG signals to a great extent.

We propose a new framework consisting of four key procedures, Singular Spectrum Analysis, Real-time Clustering, Frequency Points Selection and Prediction, Multiple-way Selection. Firstly, we introduce Singular Spectrum Analysis to decompose the PPG signals and extract its main subcomponents, among which are the heart rate subcomponents, motion artifacts subcomponents and others. Secondly, we propose Real-time Clustering to remove the subcomponents discontinuous in time domain and help to extract the skeleton of the subcomponents, which gives guidance for the selection and prediction of next step. Thirdly, we propose Frequency Points Selection and Prediction to classify the subcomponents into HR subcomponents and noise subcomponents. In this way, we can get the HR information from heart rate subcomponents. Finally, we introduce a Multiple-way Selection method to improve the robustness of the framework, which performs remedial measure promptly when the algorithm realizes it has lost the tracking of HR.

Experiments of this work are based on the datasets recorded from 12 subjects [14]. In these datasets, three kinds of singals was recorded when the subjects were running at the top speed of 15km/h, sampled at 125Hz.The signals include two-channel PPG signals, three-axis acceleration signals, and one-channel ECG.

In the following, there are 4 sections. Section II shows the problems addressed in this paper and the motivation. Section III shows the details of the proposed framework. In section IV we describe the experiment and result of the proposed framework in contrast with TROIKA Algorithm [14]. In section V, we make a conclusion of this work, and give a description about the future work.

II. Problems and Motivations

PPG waveform consists of a pulsatile physiological waveform ('AC'), a component in low frequency caused by respiration, sympathetic nervous system activity and thermoregulation ('DC') [18], shown in Figure 1. Pulsatile physiological waveform contains heart rate (HR) information we are interested in. Based on the prior knowledge, we know pulsatile physiological waveform can be regard as a periodic signal in a certain time window. Therefore, analysis in frequency domain is efficient, and little attention is paid to the DC components.

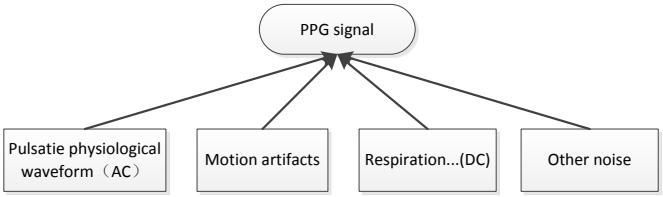

Fig. 1. PPG Composition

To analyze signal in frequency domain, the periodogram is widely adopted. Periodogram is achieved by Fast Fourier Transform (FFT) [18]. However, periodogram has high variance and serious leakage effect. Leakage effect means when motion artifacts components and pulse components are superimposed, and their frequency peaks are close, an incorrect peak may occur in the periodogram [1]. Therefore, periodogram could not be used directly in this case. However, when we decompose the superposed signals into subcomponents sparse in frequency domain, the leakage of FFT seldom occurs, and then FFT can get a good performance. Thus, we introduce Singular Spectrum Analysis (SSA) to decomposed the PPG signal into several subcomponents, and then we apply FFT

to every subcomponent to get its periodogram. After that, we get the peaks of these periodogram in order to fetch the main frequency points of the PPG signals.

Based on the prior knowledge of the PPG signals' composition, the frequency points from the subcomponents after SSA mainly represent the frequency of heart rate and motion artifacts. Most of the previous work remove the frequency points which are close to motion artifacts directly using the movement information from accelerators. However, we think in that way, a great number of information will be lost because the frequency of movement is almost the same as the frequency of HR in many cases. Therefore, we keep all of the frequency from PPG signals instead, and classify the frequency points with more information in the next step.

Frequency Point Selection and Prediction are performed to find out the frequency of HR from the frequency points representing HR, motion artifacts and other noise. To improve the performance, we introduce clustering [20] into this work based on the fact that HR won't change rapidly in a certain time window. Through clustering, we can find out the skeleton of these frequency points, which gives guidance to the frequency selection and prediction. In the meanwhile, the aperiodic noise will be thrown away through clustering, which achieves denoising in a certain extent.With the guidance of the clustering result, selection and prediction processing is much easier and the framework is more robust and its performance is much better.Unfortunately, clustering usually performs on unreal-time condition, so we propose a Real-time Clustering method for the framework to cater the real-time requirement.

Although the robustness is much better due to Real-time Clustering, we propose an error recovery processing, called Multiple Way, additionally. It makes this framework more reliable and more stable. Multiple Way only takes action when fatal error appears. Considering the real-time requirements, Multiple Way won't correct the former result, but just correct the error instead.

III. The proposed framework

The proposed framework contains six procedures: Bandpass Filtering, Singular Spectrum Analysis, Frequency Points Extraction, Real-time Clustering, Frequency Points Selection and Prediction, Multiple Way Selection. The total framework is shown in Figure 2. Bandpass Filtering removes noise from the raw PPG signal with prior information. Singular Spectrum Analysis decomposes the PPG signal into subcomponents in frequency domain. Real-time Clustering extracts the skeleton of subcomponents based on prior knowledge in the time domain. With the prior knowledge, Frequency Points Selection and Prediction selects the subcomponents with pulse or predict frequency to get HR information. Multiple Way Selection performs remedial measure using subcomponents information stored before, when the framework algorithm fails to track HR completely.

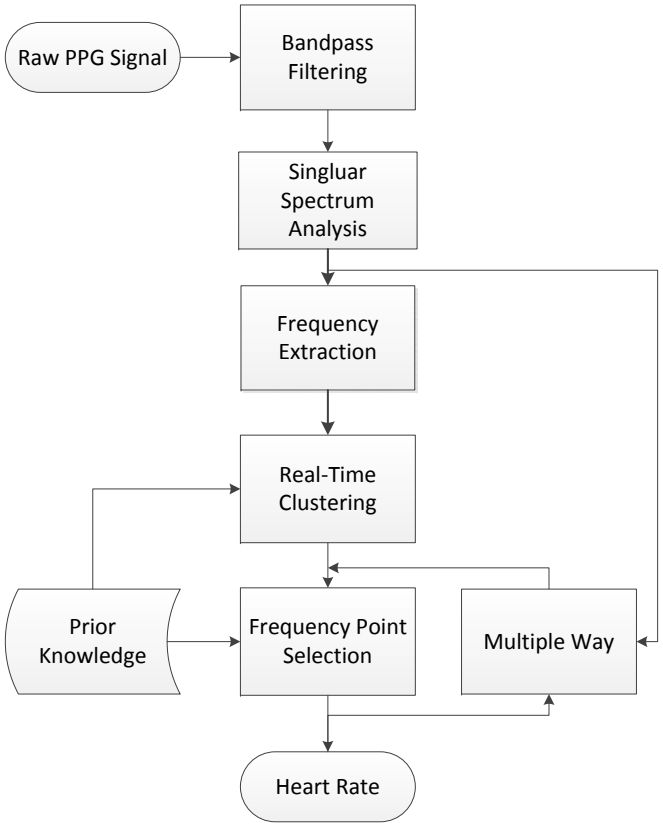

Fig. 2. The proposed framework's flowchart, in which the Singular Spectrum Analysis, Real-time Clustering, Frequency Points Selection and Prediction, Multiple Way Selection are the key parts to this framework.

A. Bandpass Filtering

Bandpass Filtering is performed on every channel of PPG signals and three-axis acceleration signals respectively to remove the noise out of the range of possible band, where HR may be located. A prior knowledge is that the HR of human beings is located from 40bpm to 190bpm [17]. So signals in the band out of this range must be noise to HR, and therefore, Butterworth IIR Filter [19] provided by MATLAB is applied to reserve the band of signals we focus on only. The Butterworth IIR Filter we use is set with parameters: order 6 and bandpass within 0.4Hz $\sim$ 5Hz.

B. SSA

Raw PPG signals are mainly affected by HR and motion artifacts. Therefore, it is valuable to decompose the raw PPG signals into subcomponents which can represent HR and movement information separately. Once subcomponents representing heart rate information are identified, we can get the HR easily.

SSA is one of the effective signal decomposition approaches [15] [16]. It can decompose signals into subcomponents as follow

$$x = \sum_{i=1}^{N} x_i \tag{1}$$

SSA is performed in four steps: embedding, singular value decomposition (SVD), grouping and diagonal averaging.

Embedding constructs the signal series $x = [x_1, \ldots, x_N]$ into an $L \times K$ trajectory matrix X which is a Hankel matrix

$$X = \begin{bmatrix} x_1 & x_2 & x_3 & \cdots & x_k \\ x_2 & x_3 & x_4 & \cdots & x_{k+1} \\ x_3 & x_4 & x_5 & \cdots & x_{k+2} \\ \vdots & \vdots & \vdots & \ddots & \vdots \\ x_L & x_{L+1} & x_{L+2} & \cdots & x_N \end{bmatrix} \tag{2}$$

SVD decomposes the trajectory matrix X in the form

$$X = \sum_{i=1}^{N} X_i \tag{3}$$

where $X_i = \sqrt{\lambda_i} U_i V_i$, $\lambda_1, \ldots, \lambda_L$ are the eigenvalues of $S = XX^T$, vector U_i is the matrix X's left singular vector and $\sqrt{\lambda_i}$ is the singular value. A golden rule to us is that a bigger singular value $\sqrt{\lambda_i}$ means the subcomponent related to this singular value contributes more to the original signal. Based on this rule, we can set the singular values as the weight to each subcomponent.

Grouping processing is used to select the subcomponents needed to be reconstructed into a group. For instance, choose N subcomponents from decomposed subcomponents into group G and mark these subcomponents with $G_1, \ldots, G_2$, and the grouped matrix $X_G = X_{G_1} + \ldots + X_{G_N}$.

Diagonal averaging can reconstruct the signal from the subcomponents. Using the one-to-one correspondence between Hankel matrices and time series can make a transformation from X_{G_k} to $\widetilde{x^{(k)}} = (x_1^{(k)}, \ldots, x_N^{(k)})$. Thus, the subcomponents in group G are constructed by

$$x_n = \sum_{k=1}^{m} \widetilde{x}_n^{(k)} \quad (n = 1, 2, \cdots, N) \tag{4}$$

In this framework, SSA is performed to decompose the two channels of PPG signals during time window T, into subcomponents which are associated with pulse, motion artifacts and others, shown as Figure 3. The top four subcomponents ordered by its singular values of each channel are used to be reconstructed by itself in our framework. That is to say, every subcomponent associated with top 4 eigenvalues is set into a group respectively, and then is reconstructed to a time serious with the same length as the input signals. Therefore, every input signal from PPG signal in a certain time windows can be decomposed into 4*2=8 main subcomponents of the time-domain signals after SSA, shown in algorithm 1.

In our experiment, the time window T is set to be 8s, considering the physiological characteristics of human beings.

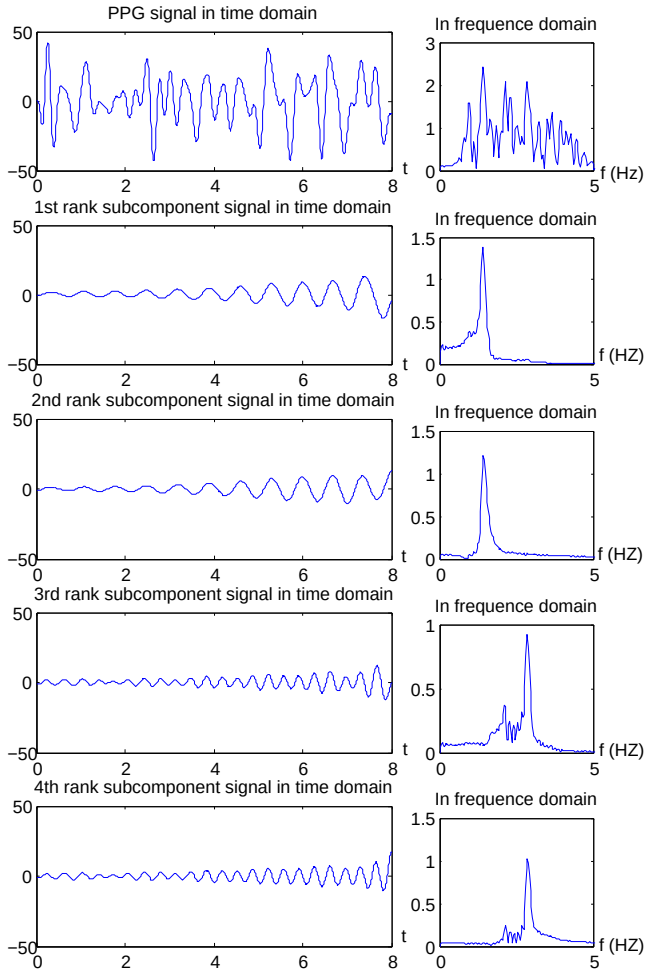

Fig. 3. SSA is performed to decompose the PPG signal of Subject 2 in time window $T = 8s$ from $0s$ to $8s$. According to the rank of singular values, the PPG signal is decomposed into top 4 subcomponents. Both the time domain and frequency domain diagrams are shown.

Algorithm 1 SSA

Input: PPG signal ppg_series in time window T.
Build trajectory matrix $X = ppg\_series.build()$
SVD $[U, autoval] = X.decompose()$
for all channel in PPG_channels **do**
  for $i = 1 \rightarrow k$ **do**
    Group $group\_sets[i] = bulidgroup(i)$
  end for
end for
for all $group \in group\_sets$ **do**
  Reconstruct $sub\_series = reconstruct(U(group))$
end for
Output: Top k sub_series by singular values $autoval$

C. Frequency Extraction

After SSA operation, every PPG signal in time window has its main subcomponents. We perform FFT to each subcomponent to get the periodogram, and then find out the peaks of the periodogram as the main frequency points of this PPG signal. First, we find out the maximum peak in the periodogram and record its amplitude P_{amp_ref} as the reference value. Next, we extract frequency points from the peaks where its amplitude $P_{amp} < 2/3 * P_{amp\_ref}$. Then we check the number of frequency points N_{points} for each subcomponent. If $N_{points} > 3$, we consider this subcomponent an aperiodic one which is unlikely to contain HR information, so we throw it away. Finally, We collect frequency points from main subcomponents. These frequency points are regarded as the main frequency of the original PPG signal.

D. Real-time Clustering

Clustering in this work is used to group the similar frequency points in adjacent time points based on the prior information that HR is impossible to change rapidly in adjacent time. In time direction, frequency points representing HR tend to be a link, so single-link clustering is suitable to do this work [21]. Furthermore, to meet the real-time requirement, we propose an improved single-link clustering method to achieve real-time clustering, where only the previous frequency points information is taken into account, and the new frequency points are clustered iteratively.

Algorithm 2 Real-time Clustering

1: **Input:** frequency points set fp_set and last frequency points set $last\_fp\_set$.
2: **if** fp is not closed to accelerometer frequency **then**
3: **for all** $fp \in fp\_set$ **do**
4: **for all** $last\_fp \in last\_fp\_set$ **do**
5: **if** $abs(fp - last\_fp) < neighbour\_dis$ **then**
6: Inherit cluster $lp.cluster+ = last.cluster$
7: **end if**
8: **end for**
9: **end for**
10: **if** $fp.cluster == null$ **then**
11: $fp.cluster = newcluster()$
12: **end if**
13: **end if**
14: **Output:** frequency points' cluster information

Algorithm 2 summarizes the proposed Real-time Clustering. Each new frequency point will inherit all cluster information from all its neighbors. Given two frequency points p_1 and p_2, the neighbor is defined by the absolute distance between the two frequency points $abs(p_1 - p_2)$. In this experiment, maximum frequency distance of two neighbor points distance is set as $neighbor\_dis = 4/60$. If there is no neighbor to a frequency point, a new cluster will be created and assigned to this point. Note that a frequency point may belong to several clusters. The information from triaxial accelerometer is also considered in the proposed Real-time Clustering. If the new frequency point is closed to the frequency of acceleration signals, which are related to motion artifacts, this point will not be put into the clustering operation. We can know whether a cluster is the skeleton to all frequency points with the size of the cluster.

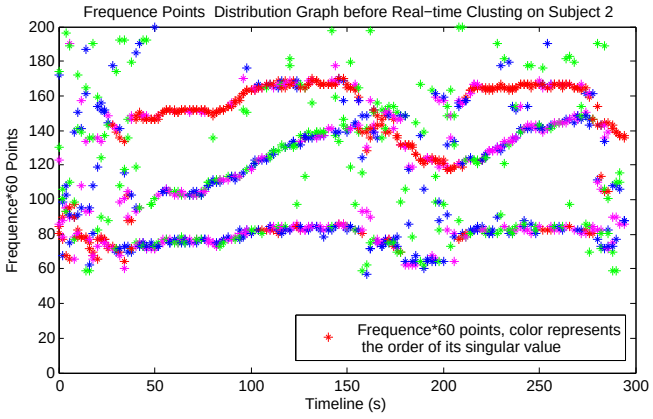

(a)

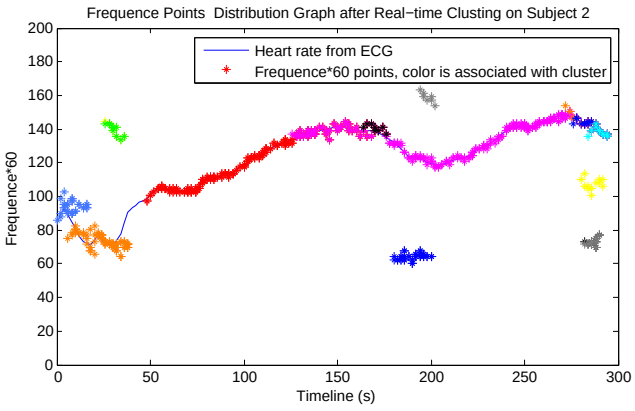

(b)

Fig. 4. The Result of Real-time Clustering

The effect of Real-time Clustering is shown clearly in Figure 4. Note that the vertical axis is $frequency * 60$ in order to be adaptive to the heartbeat unit. The distribution of the frequency points related to main subcomponents from Frequency Extraction are plotted in Figure 4(a). It contains much noise including strong motion artifacts and other noise. Figure 4(a) reveals the result of Real-time Clustering. The single HR link is much more clear without the interference of motion artifacts and other noise. Real-time Clustering achieves a good performance in this work.

E. Frequency Point Selection and Prediction

Frequency Point Selection and Prediction is a significant part of our algorithm. The algorithm is based on the common sense that HR value in two successive time window are very close.

Through the SSA, initially, we get the top twenty subcomponents of PPG signal in every time window related to

singular values which may be used to calculate or estimate the HR. However, we only use the top four subcomponents in this algorithm. On one hand, our experiments show that in most cases, the top four subcomponents have already provided sufficient information for Frequency point selection and prediction. On the other hand, this can greatly reduce the complexity of the algorithm.

The Frequency Point Selection and Prediction algorithm consists of two parts: initialization, subcomponents selection and prediction.

1) Initialization: At the initialization stage, we need to get the HR of the first three time windows as accurate as possible. We give top priority to the first rank subcomponents of both PPG1 and PPG2. If failed, then the components that rank second or third are taken into consideration. If all these selection failed, then the HR will be set at 90 BPM.

In application, users will be asked to avoid hand motion at the initialization stage, so the statistics will be much more precise.

Let the x-th channel of PPG signal be denoted by PPG_x, the i-th subcomponents of PPG be denoted by i. The frequency of the i-th subcomponents of PPG_x is denoted by $V_x(i)$. Then the algorithm can be shown in Algorithm 3.

Algorithm 3 Initialization of Frequency Point Selection and Prediction

Input: $V_x(i)$.
for index=1:4 **do**
  if $in\_region(V_{PPG1}(i))$ **then**
    $HR = V_{PPG1}(i))$
    return
  end if
  if $in\_region(V_{PPG2}(i))$ **then**
    $HR = V_{PPG2}(i))$
    return
  end if
end for
$HR = 90$
Output: HR

2) Subcomponents selection and prediction: Let the last time window be denoted by N_{prev}, and the window before N_{prev} be denoted by N_{former}. Then the gradient of the present time window $\sigma = N_{former} - N_{prev}$.If the variation tendency of HR is consistent with the gradient, then HR in this window should be $P_{obey} = N_{prev} + \sigma$. Otherwise, the HR in this window should be $P_{oppo} = N_{prev} - \sigma$.

The following actions are taken for PPG1 and PPG2 respectively:

In order to find which direction to take, two matrixes are build: M_{pos} stores the indexes of those positive subcomponent while M_{neg} stores the indexes of those negative subcomponents. First, we traverse the top four subcomponents near P_{obbey}. Next, the index of the subcomponents being traversed whose value is different from the accelerometer, and whose distance to P_{obbey} is less than Δs at the same time, will be stored in M_{pos}. After that, the same operation will be taken to the top four subcomponents near P_{oppo}, and the result will be stored in M_{neg}. In our algorithm, the important parameter Δs is valued in equation: $\Delta s = 3.5 + M_{weight\_set(i)}$, where M_{weight_set} is a matrix carrying the weight of all components, and i denotes the index of the component.

During this process, the index of the components being traversed which are overlapped with accelerometer, and whose distance to N_{former} is less than Δs at the same time, are stored in matrix M_{cwa} (coincide with accelerometer). In the meanwhile, the index of the components being traversed whose value is different from the accelerometer, and whose distance to N_{prev} is less than Δd at the same time, are stored in matrix M_{ctnp} (close to N_{prev}). In our algorithm, Δd is set at 40 BPM.

Algorithm 4 Subcomponents Selection and Prediction

Input: M_{pos},M_{neg}, M_{cwa}, M_{cwnp}, $M_{cluster\_info}$
$record = [is\_empty(pos1; is\_empty(pos2;$
$is\_empty(neg1); is\_empty(neg2)]$
for index=1:4 **do**
  if $record(i) == 0$ **then**
    $HR = calculate.average(i)$
    $return$
  end if
end for
$addr = min(abs(cluster\_info - N_{prev}))$
if $abs(cluster\_info(addr) - N_{prev}) < \Delta d1$ **then**
  if $HR = cluster\_info(addr) - N_{prev} > 0$ **then**
    $HR = N_{prev} + \Delta d2$
  else
    $HR = N_{prev} - \Delta d2$
  end if
else if $length(M_{cwa}) >= 2$ && $M_{cwa}(1,2) <= 3$ **then**
  $HR = M_{cwa}(1,1)$
else if $is\_empty(M_{cwnp})$ **then**
  $HR = N_{prev}$
else
  if $\sum_{\forall V_x(i) > N_{prev}} weight(i) > \sum_{\forall V_x(i) > N_{prev}} weight(i)$ **then**
    $HR = N_{prev} + \Delta step$
  else
    $HR = N_{prev} - \Delta step$
  end if
end if
Output: HR

There are four cases after the traversal, shown in Algorithm 4.

Case 1: If matrixes M_{pos} and M_{neg} for both PPG1 and PPG2 are empty, then the algorithm jumps to Case 2. Otherwise, use the non-empty matrixes to get the HR by calculating the average frequency of the indexes stored in them.

Case 2: If the clustering set is empty, then jump to Case 3. Otherwise, find the closest frequency $f_{closest}$ from the clustering set. Denote the distance between $f_{closest}$ and N_{prev} as d and give parameter $\Delta d1 = 22.4$, $\Delta d2 = 9.6$. If d is less than $\Delta d1$, than $HR = N_{prev} \pm \Delta d2$. If $f_{closest}$ is larger than N_{prev}, then $HR = N_{prev} + \Delta d2$.

Case 3: This step is designed to determine HR when the BPM value overlaps with the the acceleration. In most cases, when matrix M_{cwa} has more than two elements and the index of the second element is no more than 3, it can be concluded that the BPM value overlaps with acceleration. Then we will obtain HR from M_{cwa} directly.

Case 4: If matrix M_{cwnp} is empty, it means that we get little information to determine HR, so we set $HR = N_{prev}$. Otherwise, we sum up the weight of ALL the components which are larger than HR or less than HR separately, and take $\Delta step$, based on N_{prev}, to the direction that has the bigger weight-sum. In our algorithm, $\Delta step = 4.8$.

F. Multiple-way Selection

Considering that the former methods select the possible HR in the current time window, according to not only the signal in the current time window, but also the HR estimated in the previous one or two time windows, a wrong estimated HR may have significant influence on the following HR selection and lead our prediction of the HR to an incorrect direction. Since the prediction is continuous (based on the fact that HR won' t change rapidly in a certain time window), once we choose several wrong frequencies which are interfered by the strong and continuous motion artifacts, we may be far away from the true HR and will never get back. It can be considered as a fatal error in HR monitoring.

In order to get rid of this fatal error, the Multiple-way Selection Method deploys multiple ways to trace all the possible HR instead of tracing only the most possible HR. The Multiple-way Selection has one or more trajectories in one time window. The most reliable frequency calculated from all the trajectories in the current time window is chosen to be the estimated HR in the current time window. The reliability of one frequency is evaluated from many aspects. The details of the method are given as follow.

1) Select current trajectory's frequency: The frequencies of each trajectory in the current time window is calculated mainly use the Frequency Point Selection and Prediction. Although the Multiple-way Selection is running in every time window, its results are used only when the estimated frequency is considered to be unreliable and may lead to an error way, such as when the frequency is generated from prediction or near the acceleration frequencies.

2) Split into several trajectories: When one trajectory has more than one possible frequencies, the trajectory is divided into several trajectories. The new trajectories inherit the reliability value from the old trajectory and regard the old trajectory as their parent trajectory. The parent trajectory is used to get the frequencies in the previous time window in the Frequency Point Selection and Prediction section. To reduce the complexity, trajectories that have the same frequency will be merged into one trajectory.

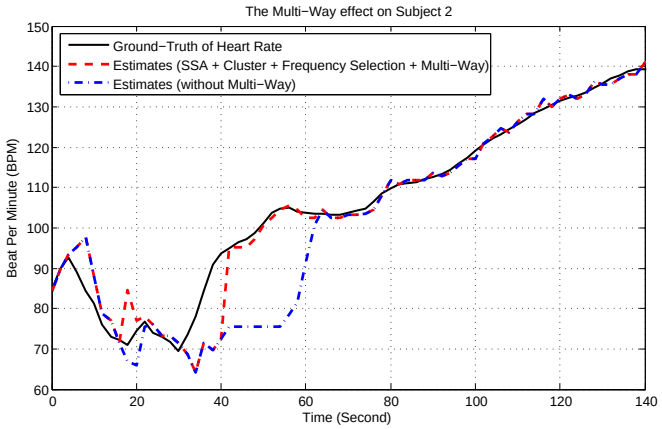

Fig. 5. It shows the effect of Multiple-way Selection. If the algorithm miss the tracking of ground-truth HR, this process may deal with error as soon as possible. With Multiple-way Selection, the global error decreases.

3) Choose the most reliable frequency: The last part is to choose the most reliable frequency in the current time window. The trajectory's reliability is set to be the reliability value of the frequency in the trajectory. The initial value of the trajectory's reliability is 0. When the trajectory generates a frequency based on prediction, the reliability value will be increased by 1. The higher reliability value is, the more unreliable the trajectory is. If there is a trajectory which has a lower reliability value than the current trajectory, the frequency in the trajectory is chosen as the final result of the Multiple-way Selection. The result is used only when the frequency in step 1 is calculated from prediction.

The Multiple-way Selection could correct estimated HR in the current time window to a more reliable value, and reduce the possibility of failure when the real HR chooses a wrong frequency. Figure 5 shows the result after implementing the Multiple-way Selection.

IV. Experiment

In this section, we describe the experiment we have done for the proposed framework. Details and results of the experiment are shown.

A. Experiment Design

Firstly, to present the framework's performance, we apply the proposed framework to 12 datasets provided by TROIKA [14] and show the result comparing with the ground truth HR from ECG signal.

Secondly, to show the effect of each part, we design a comparison test for the framework itself. We remove each part separately and show the difference of results between each other.

Finally, we perform a comparison test with TROIKA, which is one of the best frameworks at present for the PPG signal during intensive physical exercise.

TABLE I

THE RESULT OF COMPARISON TESTS ON 12 DATASETS IN SEVERAL CONDITIONS: THE COMPLETE PROPOSED FRAMEWORK, FRAMEWORK WITHOUT MULTI-WAY (MW), FRAMEWORK WITHOUT REAL-TIME CLUSTERING (RC), AND FRAMEWORK WITHOUT EITHER MULTI-WAY (MW) OR REAL-TIME CLUSTERING (RC).

Algorithm Item	Subj 1	Subj 2	Subj 3	Subj 4	Subj 5	Subj 6	Subj 7	Subj 8	Subj 9	Subj 10	Subj 11	Subj 12
The porposed Framework	1.58	2.25	0.99	1.91	1.47	2.21	1.07	0.97	0.94	4.91	1.71	1.94
Framework without MW	1.70	2.36	1.00	2.14	0.87	1.96	1.01	0.73	0.86	8.93	1.15	1.88
Framework without RC	1.66	2.66	0.97	2.03	0.88	2.65	0.99	1.24	0.96	36.55	21.15	2.04
Framework without MW&RC	6.07	3.17	1.46	1.98	1.12	54.60	1.28	0.73	0.69	44.65	41.15	2.67

TABLE II

ABSOLUTELY ERROR RESULT COMPARISON TO TROIKA

Algorithm Item	Subj 1	Subj 2	Subj 3	Subj 4	Subj 5	Subj 6	Subj 7	Subj 8	Subj 9	Subj 10	Subj 11	Subj 12
The porposed Framework	1.58	2.25	0.99	1.91	1.47	2.21	1.07	0.97	0.94	4.91	1.71	1.94
TROIKA	2.29	2.19	2.00	2.15	2.01	2.76	1.67	1.93	1.86	4.70	1.72	2.84

TABLE III

RESULT COMPARISON WITH ERROR PERCENTAGE

Algorithm Item	Subj 1	Subj 2	Subj 3	Subj 4	Subj 5	Subj 6	Subj 7	Subj 8	Subj 9	Subj 10	Subj 11	Subj 12
The porposed Framework	1.39%	2.41%	0.82%	1.77%	1.06%	1.83%	0.79%	0.83%	0.75%	3.18%	1.12%	1.38%
TROIKA	1.90%	1.87%	1.66%	1.82%	1.49%	2.25%	1.26%	1.62%	1.59%	2.93%	1.15%	1.99%

In this experiment, we use average absolute error Err_{ab} and average relative error Err_{re} to estimate the performance of the result. Denote by $BPM_{real}(i)$, the $i-$th real HR from ECG, and denote by $BPM(i)$, the $i-$th estimate result. The average absolute error is defined as

$$Err_{ab} = \frac{1}{N}\sum_{k=1}^{N}|BPM(i) - BPM_{real}(i)| \tag{5}$$

The average relative error is defined as

$$Err_{re} = \frac{1}{N}\sum_{k=1}^{N}\frac{|BPM(i) - BPM_{real}(i)|}{BPM_{real}(i)} \tag{6}$$

B. Datasets Description

Datasets contain two channels PPG signals and triaxial accelerometer signals sampled at 125Hz. What's more, datasets also contain ECG signals regarded as ground truth heart rate for the estimation. Datasets are recorded from 12 subjects with changing speed, aged from 18 to 35. The maximum speed is up to 15km/h, in which condition motion artifacts affect PPG signals seriously. Both pulse oximeter and accelerometer are embedded in wristband.

C. Results

As it is described in the Experiment design part, we implement different parts of the new proposed framework on the same subject, and we have various results as it is showed in the Figure 6 and Figure 7.

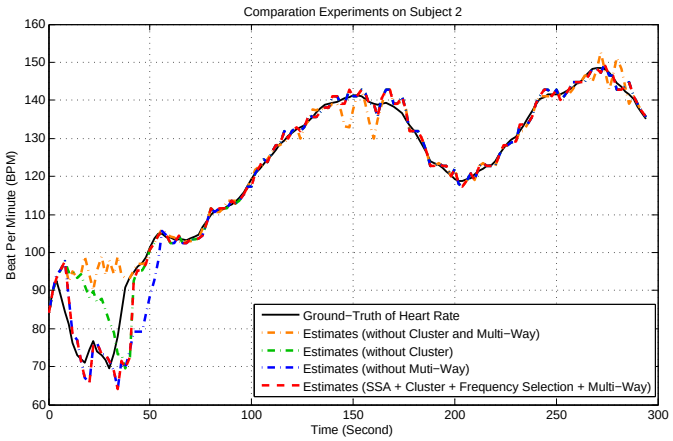

Fig. 6. Comparison experiments have been done to show the importance of each part in our proposed framework. This figure shows the result of HR tracking on Subject 2 in four cases: the complete framework (SSA+Clustering+Frequency Selection+Multi-Way), framework without Clustering, framework without Multi-May, framework without either Real-time Clustering or Multi-May. In the figure, the ground truth HR is also plotted as a reference.

Without Cluster and Multiple-way Selection, the estimated HR will go straight and it means that the algorithm has missed the tracking of the HR. In the following procession,

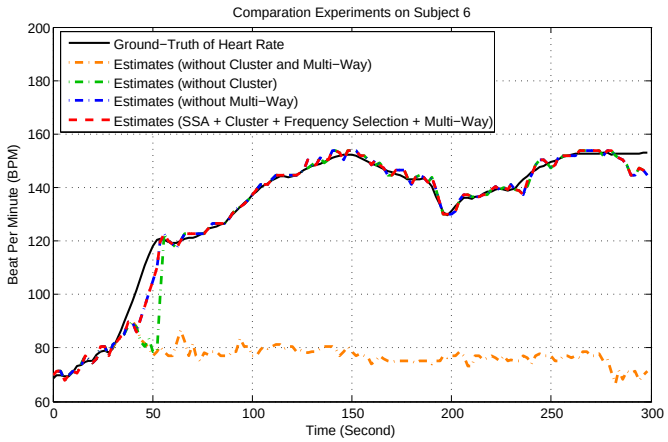

Fig. 7. Another comparison experiment on the framework with different parts has been done in different cases on Subject 3.

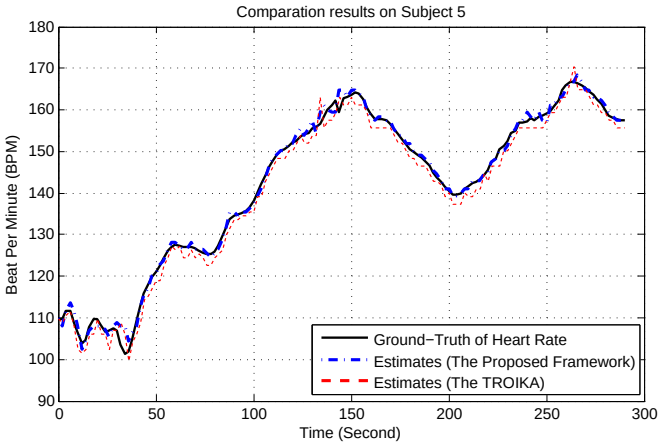

Fig. 8. Comparison test with TROIKA on Subject 5. The result of TROIKA is from its paper [14], shown with the red line.

the algorithm almost get the result randomly, and it only can get back to track the ground-truth HR by chance. It is not robust.

With the Real-time Clustering, algorithm can get the ground-truth HR with the guidance of the skeleton from cluster information. It can deal with most of terrible cases, and it make the framework much more robust.

After adding Multi-Way, the estimated HR can follow up to the true HR after about 30 seconds when the current trajectory is considered to be unreliable. When only the Multi-Way is absent, the estimated HR have difficult in keeping up with the true HR since there is a steep rise and the estimated HR delayed almost 10 seconds. Including all the four parts of the new proposed framework performs the best and it has an extraordinary remarkable effect during the steep rise and fall.

To show the contribution of the proposed framework to the PPG signal processing, we have done comparison tests to TROIKA, which is one of the most efficient algorithm at present. We apply our proposed framework to the same

Fig. 9. Comparison test with TROIKA on Subject 6. The result of TROIKA is from its paper [14], shown with the red line.

datasets as the TROIKA use. We get the result of TROIKA on the 12 datasets from its paper.

Figure 8 and Figure 9 show the performances of both our proposed framework and TROIKA on Subject 5 and Subject 6. We can see both the algorithms can tracking the HR, referring the ground-truth HR. And for details, it can been seen that the proposed framework has higher precision in both datasets.

Besides the Subject 5 and Subject 6, another 10 datasets are also used in the experiment to show the robustness of the framework. Table II represents the average absolute error on all the 12 subjects while Table III lists the average relative error. From the tables, we can see that the proposed framework can tracking the HR in all of the datasets with global error under 5 BPM , so does the TROIKA. Compared with TROIKA, the proposed framework get a better performance in most of the cases. Furthermore, the proposed framework decreases more than 50% of the absolutely error in contrast with TROIKA on subject 3, 8 and 9.

V. Conclusion and Future Work

In this paper, we focus on the HR information extraction from PPG signals with strong motion artifacts. We proposed a new framework to deal with this task. The framework contains four key parts:Singular Spectrum Analysis for signal decomposition, Real-time Clustering for skeleton extraction, frequency selection and prediction for HR information judgement, Multiple-way Selection for quality guarantee.

Experiments are conducted based on the 12 datasets and the framework performs well in terms of robustness and precision. We also make a comparison with TROIKA, which is a good framework on the same task, and we get a better result in most cases.

In the future, we will focus on the computational complexity in order to make this framework more applicable to the wearable devices. In this paper, robustness and precision are emphasized, while the efficiency of the algorithm still can be

improved. And we believe that this work is still valuable to wearable devices and mobile telemedicine.

REFERENCES

[1] Allen J. Photoplethysmography and its application in clinical physiological measurement[J]. Physiological measurement, 2007, 28(3): R1.

[2] López S M, Giannetti R, Dotor M L, et al. Heuristic algorithm for photoplethysmographic heart rate tracking during maximal exercise test[J]. 2012.

[3] Yan Y, Poon C C Y, Zhang Y. Journal of NeuroEngineering and Rehabilitation[J]. Journal of NeuroEngineering and Rehabilitation, 2005, 2: 3.

[4] Diab M K, Kiani-Azarbayjany E, Elfadel I M, et al. Signal processing apparatus: U.S. Patent 8,755,856[P]. 2014-6-17.

[5] Matthews G R. Pulse responsive device[J]. International Patent Application WO 91, 1991, 18550.

[6] Parker D. Optical monitor (oximeter, etc) with motion artifact suppression[J]. International Patent Application WO 94, 1994, 3102.

[7] Hayes M J, Smith P R. Artifact reduction in photoplethysmography[J]. Applied Optics, 1998, 37(31): 7437-7446.

[8] Hayes M J, Smith P R. A new method for pulse oximetry possessing inherent insensitivity to artifact[J]. Biomedical Engineering, IEEE Transactions on, 2001, 48(4): 452-461.

[9] Swedlow D B, Potratz R S. Oximeter with motion detection for alarm modification: U.S. Patent 5,368,026[P]. 1994-11-29.

[10] Yousefi R, Nourani M, Ostadabbas S, et al. A motion-tolerant adaptive algorithm for wearable photoplethysmographic biosensors[J]. Biomedical and Health Informatics, IEEE Journal of, 2014, 18(2): 670-681.

[11] Han H, Kim M J, Kim J. Development of real-time motion artifact reduction algorithm for a wearable photoplethysmography[C]//Engineering in Medicine and Biology Society, 2007. EMBS 2007. 29th Annual International Conference of the IEEE. IEEE, 2007: 1538-1541.

[12] Asada H H, Jiang H H, Gibbs P. Active noise cancellation using MEMS accelerometers for motion-tolerant wearable bio-sensors[C]//Engineering in Medicine and Biology Society, 2004. IEMBS'04. 26th Annual International Conference of the IEEE. IEEE, 2004, 1: 2157-2160.

[13] Ram M R, Madhav K V, Krishna E H, et al. A novel approach for motion artifact reduction in PPG signals based on AS-LMS adaptive filter[J]. Instrumentation and Measurement, IEEE Transactions on, 2012, 61(5): 1445-1457.

[14] Zhang Z, Pi Z, Liu B. TROIKA: A General Framework for Heart Rate Monitoring Using Wrist-Type Photoplethysmographic (PPG) Signals During Intensive Physical Exercise[J]. 2014.

[15] N. Golyandina, V. Nekrutkin, and A. A. Zhigljavsky, Analysis of time series structure: SSA and related techniques. CRC Press, 2001.

[16] T. Harris and H. Yuan, "Filtering and frequency interpretations of singular spectrum analysis," Physica D: Nonlinear Phenomena, vol. 239, no. 20, pp. 1958 – 1967, 2010.

[17] Kligfield P, Ameisen O, Okin P M. Heart rate adjustment of ST segment depression for improved detection of coronary artery disease[J]. Circulation, 1989, 79(2): 245-255.

[18] J. Allen, Photoplethysmography and its application in clinical physiological measurement, Physiological Measurement, vol. 28, no. 3, pp. R1-R39, 2007

[19] Butterworth S. On the theory of filter amplifiers[J]. Wireless Engineer, 1930, 7(6): 536-541.

[20] Murtagh F, Contreras P. Algorithms for hierarchical clustering: an overview[J]. Wiley Interdisciplinary Reviews: Data Mining and Knowledge Discovery, 2012, 2(1): 86-97.

[21] Patra B K, Nandi S. Fast single-link clustering method based on tolerance rough set model[M]//Rough Sets, Fuzzy Sets, Data Mining and Granular Computing. Springer Berlin Heidelberg, 2009: 414-422.